

Sleeve forces on inclined cylinders due to long and short crested waves

Les forces exercées sur les cylindres inclinés par les vagues longues et courtes.

V. SUNDAR, *Department of Ocean Engineering, Indian Institute of Technology Madras, India*

V. VENGATESAN, *Formerly with Department of Ocean Engineering, Indian Institute of Technology Madras, India and presently with Department of Naval Architecture and Ocean Engineering University of Edinburg, United Kingdom*

K.U. GRAW, *Department of civil Engineering, University of Leipzig, Germany*

ABSTRACT

The wave-induced pressures around an inclined cylinder due to long and short crested waves are measured in a wave basin at an elevation of 0.8 m below still water level in a water depth of 3 m. The sleeve force normal to the cylinder axis was obtained by integrating the circumferential pressures and resolved in each of the three directions. The variations of the spectral density of the sleeve forces are presented. The effects of wave directionality on the pressures and sleeve forces are presented in the form of root mean square pressure and force ratios defined as normalized root mean square pressures / forces in short crested waves to that in long crested waves. The variations of the pressure and force ratios are discussed for the different mean wave directions and for different angles of inclinations of the cylinder with respect to the vertical plane. The pressure ratio is observed to be minimum when it is inclined at 45° along the wave direction. The maximum normal force ratio is about 25 to 37% less when cylinder is exposed to directional waves compared to being subjected to long crested waves.

RÉSUMÉ

On mesure dans un bassin à houle les pressions exercées sur un cylindre incliné par des vagues longues et courtes ; le bassin a une profondeur de 3 m, la mesure est effectuée à 0.8 m sous le niveau libre. La force normale à l'axe du cylindre a été obtenue en intégrant les pressions circonférentielles, et résolue dans chacune des trois directions. On présente les variations de la densité spectrale des forces. L'effet directionnel de la houle sur les pressions et les forces est présenté sous la forme d'une valeur quadratique moyenne de rapports de pression et de force définis comme la valeur quadratique moyenne normalisée des pressions / forces dans les vagues courtes rapportée à celle observée dans les vagues longues. Les variations des rapports de pression et de force sont discutées pour les différentes directions moyennes de houle et pour différents angles d'inclinaison du cylindre par rapport au plan vertical. Le rapport de pression est minimum lorsque celui-ci est incliné à 45° dans la direction de la houle. Le rapport maximum de la force normale est environ de 25 à 37% moins élevé lorsque le cylindre est exposé à des houles directionnelles que lorsqu'il est soumis à des vagues longues.

Keywords: Sleeve forces, Dynamic pressures, Short crested and Long crested waves, Directional waves, Pressure spectra, Force ratio.

1. Introduction

The topic of wave forces on slender cylinders continues to be one of the most widely investigated research problems. Inclined tubular members form integral members of a variety of marine structures and thus, studies on the forces due to waves on such structures are very important. The orientation of the cylinder can have a significant influence on the force for certain wave characteristics.

Borgman (1958) proposed the methodology for the computation of wave loads on an arbitrarily oriented cylinder using the formulation of Morison et al.(1950). Johansson (1978), through the ocean test program (OTS), reported that the scatter in the hydrodynamic coefficients for an inclined cylinder was considerably larger compared to the scatter for a vertical cylinder. Chakrabarti et al., (1977) reported experimental results for inclined tubular members in oscillatory waves in shallower water depths covering Keulegan-Carpenter, (KC) number ($u_{\max} T/D$) up to about 16. The experimental data demonstrated the dependence of coefficients of drag, C_D and inertia, C_M on the KC number and on the orientation of the cylinder.

Anandkumar et al., (1995a) have summarized the details of work carried out by different researchers on the forces on inclined cyl-

inders due to regular waves. It was concluded that the effect of the tilting angle of the cylinder on the force normal to its axis is insignificant for shorter waves, whereas its effect in long waves is quite significant. In the case of random wave tests on inclined cylinders, Anandkumar et al., (1995b) concluded that the spectral density of the normal force increases with increase in the tilting angle except when the cylinder is inclined along the wave direction at 45° from the vertical plane.

Predictions of wave loads on cylinders are traditionally based on laboratory tests in a unidirectional wave field. For real offshore conditions, the waves are multidirectional or short crested. The estimation of the wave loading in directional waves is closer to reality and, hence would lead to an optimum design resulting in considerable cost savings. The experimental studies on loading on structures due to such waves in the laboratory is limited because only a few laboratories are equipped with facilities to generate directional waves. Aage et al.(1989) studied the in-line, transverse and resultant forces on a cylinder in 2D and in 3D waves. The results were presented in the form of force ratios between 3D and 2D waves. It is reported that the statistical distribution of in-line force is identical with the resultant force and does not vary significantly with the spreading function. The in-line and resultant forces were found to be about 15 percent smaller in 3D waves

Revision received April 17, 2002. Open for discussion till October 31, 2002.

compared to in 2D waves and transverse forces were about one half of the in-line forces. Chaplin et al. (1993) in their studies on the in-line loading on a vertical cylinder have reported the reduction in in-line loading associated with directionality and also observed that the drag coefficient reduces as the wave spread increases, while the inertia and rms coefficients in multidirectional waves are not significantly different from those in unidirectional waves. Hogedal et al. (1994) conducted experiments to study the wave forces on a vertical cylinder in directional waves and confirmed the reduction in the forces due to short crested sea, the percentage reduction being dependent on the mean heading direction of the wave. The measured reduction of the wave forces was found to agree with the results from similar tests of Aage et al. (1989) and Chaplin et al. (1993) and theoretical results reported by Isaacson & Nwogu (1988). From the literature, it is noted that considerable work on the forces on cylinders due to regular and random waves has been reported whereas, that due to directional waves is rather limited. This has necessitated an experimental study on the present topic.

2. Experimental programme

A carefully-controlled experimental program was carried out in a wave basin of size 30m × 30m, in Ocean Engineering Centre, Indian Institute of Technology, Madras, India. The wave basin, with a constant water depth of 3m, is equipped with a Long crested Wave Maker (LCWM) on one and Multi-Element Wave Maker (MEWM) on the other side running normal to the LCWM. The LCWM is capable of generating only unidirectional long crested regular and random waves. The MEWM is capable of generating regular and directional random waves of predefined spectral characteristics associated with or without directional spreading of the waves referred to as short and long crested waves respectively. The MEWM consists of 52 paddles, each 0.5 m in widths, which are hinged 1.3m below the water surface and 1.7m above the basin floor. Each paddle pivots independently according to the servo-actuator motion. The front of each of the 52 paddles is covered by an elastic membrane, which ensures that the rear side of the wave makers is dry. The membrane is elastic and tolerates elongation beyond the working range of the paddles. The test cylinder of 0.2 m diameter consists of several individual segments. The test section is fixed with 12 pressure transducers around its circumference and positioned at an elevation of 0.8 m below the still water level, which was kept the same for all angles of inclinations of the cylinder. The tests were carried out in unidirectional random waves and directional waves.

The short-crested sea state was described by a 2D Pierson-Moskowitz frequency spectrum with an associated cosine square type spreading function. The spreading function was defined by three values of mean wave direction, β_o ($\beta_o = 0^\circ, 15^\circ$ and 30°), defined in Table.1 as directional waves denoted by DW1, DW2 and DW3 respectively. LCW denotes the long crested waves. The significant wave height, H_s and peak frequency, f_o adopted for the study are also given in Table.1.

Table 1. Input directional wave parameters

Run No.	H_s (m)	f_o (Hz)	β_o (deg)
LCW	0.22	0.667	-
DW1	0.15	0.667	0
DW2	0.15	0.667	15
DW3	0.15	0.667	30

Measuring the generated directional waves in the absence of a structure tested the quality of multidirectional waves in the basin. A wave gauge and a velocity probe were fixed at a distance of 8.0m from the MEWM, where the position of the model was to be installed. Each of the pressure transducers has a range of ± 0.2 bar. The diameter of the diaphragm is 10mm. The instantaneous change in the displacement of the diaphragm due to action of external pressure is proportional to the instantaneous change in applied pressure. The sensitivity of each of the transducer varies from 25.06 to 25.24 mV at about 25° . The velocity probe (minilab make) is an ultrasonic laboratory current metering system, which measures the current by transmitting acoustic signals between pairs of piezoelectric transducer probes in three orthogonal directions. The transducers are made of 4 MHz ceramic elements. The horizontal axes of the probe use reflector, while, the vertical axis uses a direct signal path. The instrumentation system consists of a three-axis probe, a probe cable, an electronic preprocessing unit in a probe house and a display unit. The probe can measure current speeds in the range of ± 1.0 m/s with a resolution of 1 mm/s and a bandwidth of 35 Hz.

The plan and sectional view of the wave basin along with the positions of the cylinder, velocity and wave probes are shown in Fig.1. Wave absorbers of parabolic section provided on either ends opposite to LCWM and MEWM effectively absorbs the incident waves. The inclination angle α is defined as the angle of inclination of the cylinder with respect to the vertical plane. The cylinder is inclined along x-direction. Positive α means the cylinder is inclined along the wave direction and negative α means the cylinder is inclined opposite to the wave direction. The wave and pressure records were collected for duration of 60 seconds with a sampling interval of 0.025 Hz. After removing the transient response, the effective record length of time series recorded was 51.2 seconds.

3. Method of analysis

The evaluation of directional waves mainly depends on the measurement of wave elevation, η , in-line particle velocity component, u and transverse particle velocity component, v . To ensure the measurements, the experimental in-line velocity, u and vertical velocity, w are compared with theoretical predictions from the measured η using the linear filter technique of Reid (1957) for a long crested waves and good agreement found as can be seen in Fig.2. The measured and computed auto spectra of in-line particle velocity, S_{uu} and vertical particle velocity, S_{ww} are also found to match reasonably as seen in Fig. 3.

A FORTRAN code DIRWAAN has been developed to analyze the multidirectional waves using the single-point measurement of

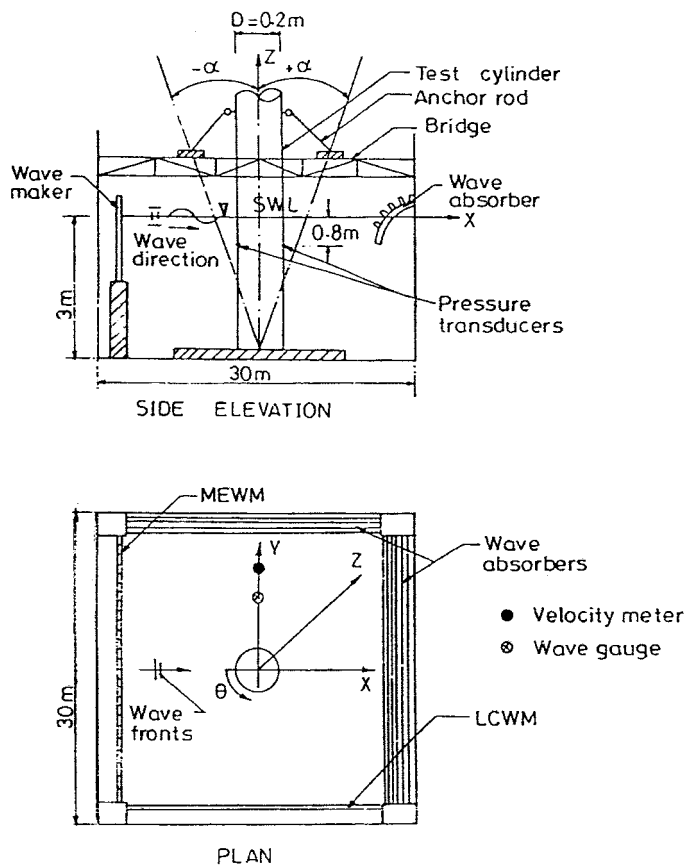


Fig. 1 Schematic sketch of the experimental setup with the model in the wave basin.

water-surface elevation and water-particle kinematics in two horizontal orthogonal directions. Three methods of Fourier series representation, FM [Sand and Mynett (1987)], Maximum Likelihood Method, MLM [Isobe et al., (1984)] and Maximum Entropy Method, MEM [Nwogu et al., (1987)] for calculating the directional spreading function, are included in the software. The spreading function is evaluated at each frequency and the directional spectrum is then calculated by multiplying with auto-spectral density of wave elevation. The salient characteristics of directional waves, spectral parameters such as peak frequency and sig-

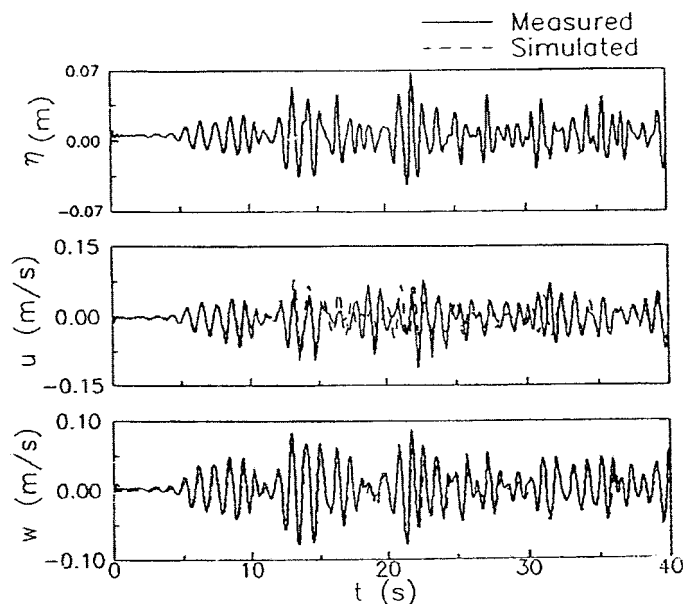


Fig. 2 Comparison of measured and predicted water particle velocities, u and w, time Series of (a) η ; (b) u (c) w.

nificant wave height and average directional parameters such as spreading index, mean wave direction and long-crestedness parameter are estimated.

The efficiency of the three methods of analysis to evaluate the directional spreading function was examined using a theoretically simulated time series for η , u and v for the directional spectrum with $s = 1$ and $\theta = 0^\circ$ [Miles (1990)]. The evaluated spreading function, $D(\omega, \beta)$ using the methods FM, MLM and MEM, is depicted in Fig. 4 along with the target spread. The comparison shows the MEM method has a higher resolution in predicting the spreading function than FM and MLM. The derived characteristics of the directional spectrum in this study, hence, are based on the MEM method.

The measured pressures around the circumference of the cylinder were integrated to obtain the normal force time histories. The normal force time history was resolved to obtain the time series of in-line, transverse and vertical forces. The time series of these

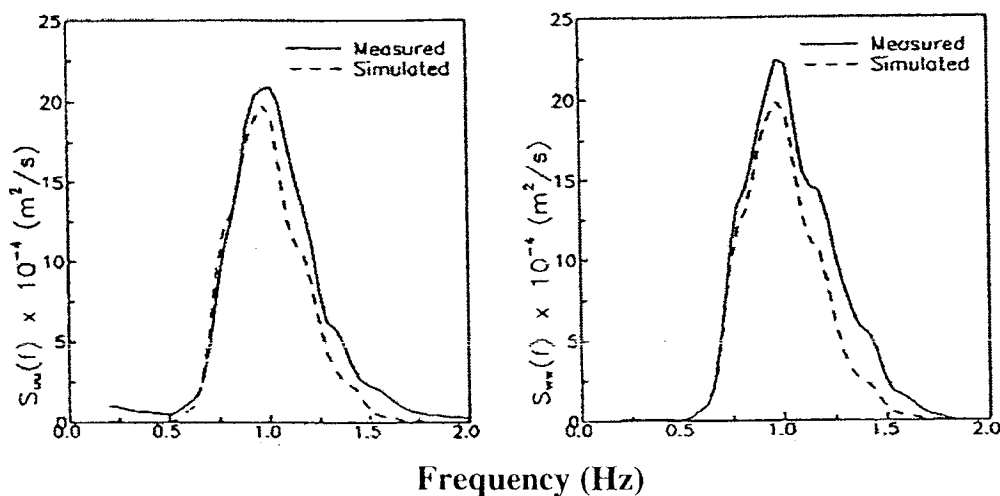


Fig. 3 Comparison of measured and predicted velocities, spectra of in-line velocity (u) and vertical velocity (w).

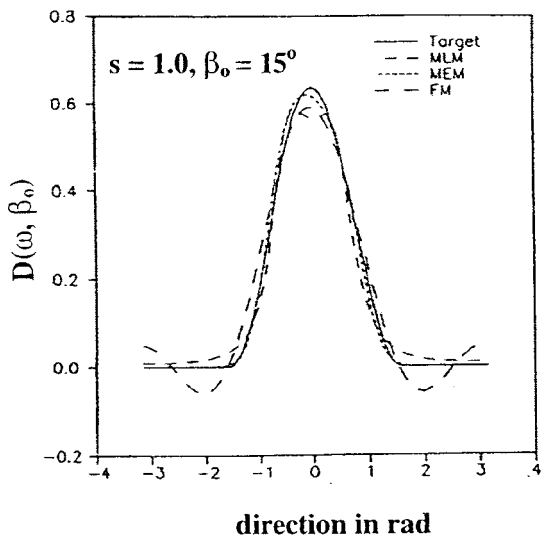


Fig. 4 Comparison of directional spread evaluated using FM, MLM and MEM with target spread.

force components were subjected to Fast Fourier Transform (FFT) analysis, to obtain the corresponding force spectra due to unidirectional and directional waves.

In order to quantify the effect of directional waves on inclined cylinders, the root mean square (rms) pressure / force in a multi-directional wave field is compared with rms pressure / force in a long crested wave field. The pressure ratio (p_r) and force ratio (f_r) are defined as the ratio of (rms pressure or force/ H_{rms}) in short crested waves to (rms pressure or forces/ H_{rms}) in long crested waves,

$$[p_r]^* = \frac{\left\{ \left[\frac{P_{rms}^*}{H_{rms}} \right]_{3D} \right\}}{\left\{ \left[\frac{P_{rms}^*}{H_{rms}} \right]_{2D} \right\}} \quad (1)$$

$$[f_r]^* = \frac{\left\{ \left[\frac{f_{rms}^*}{H_{rms}} \right]_{3D} \right\}}{\left\{ \left[\frac{f_{rms}^*}{H_{rms}} \right]_{2D} \right\}} \quad (2)$$

where "*" represents n,x,y or z for normal, in-line, transverse and vertical force respectively. Herein, 3D and 2D represent short and long crested waves respectively. The above way of representing the pressure ratios is quite advantageous since the pressure values in 3D and 2D are normalized with their corresponding significant wave heights. Hence, one need not have to simulate the same input conditions especially, the significant wave height for the 2D and 3D waves as this would be quite difficult.

4. Results and discussion

4.1 Directional Spreading Function

The measured pressures around the cylinder have been validated [Anandkumar et al., (1995a) and Sundar et al., (1998)]. A typical

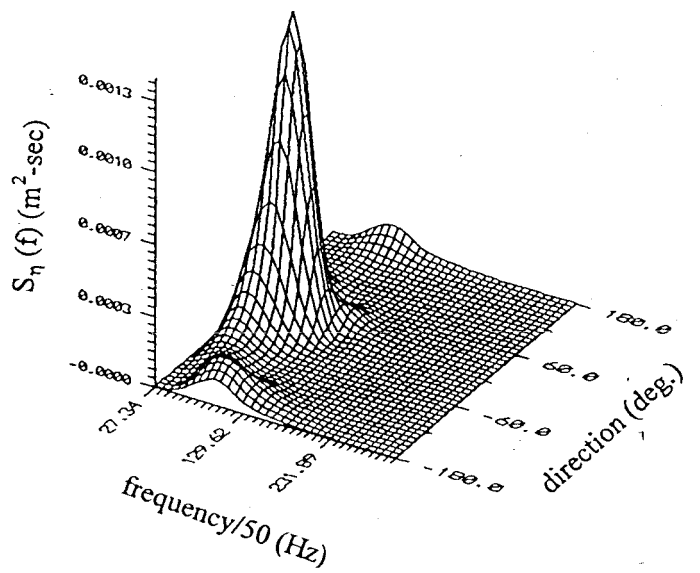


Fig. 5 Typical directional spectra.

measured directional spectrum subjected to different mean wave directions, for the test run DW2 ($\beta_0 = 15^\circ$) is depicted in Fig. 5. Typical comparisons of measured and target 2D spectrum and corresponding directional spread are shown in Fig. 6. The normalized spectral density of wave elevation $S'_\eta = [S_\eta(f) / H_s^2 T_p]$, in which $S_\eta(f)$ is spectral density of η , H_s is the significant wave height and the peak period T_p ($T_p = 1/f_0$, where, f_0 is the peak

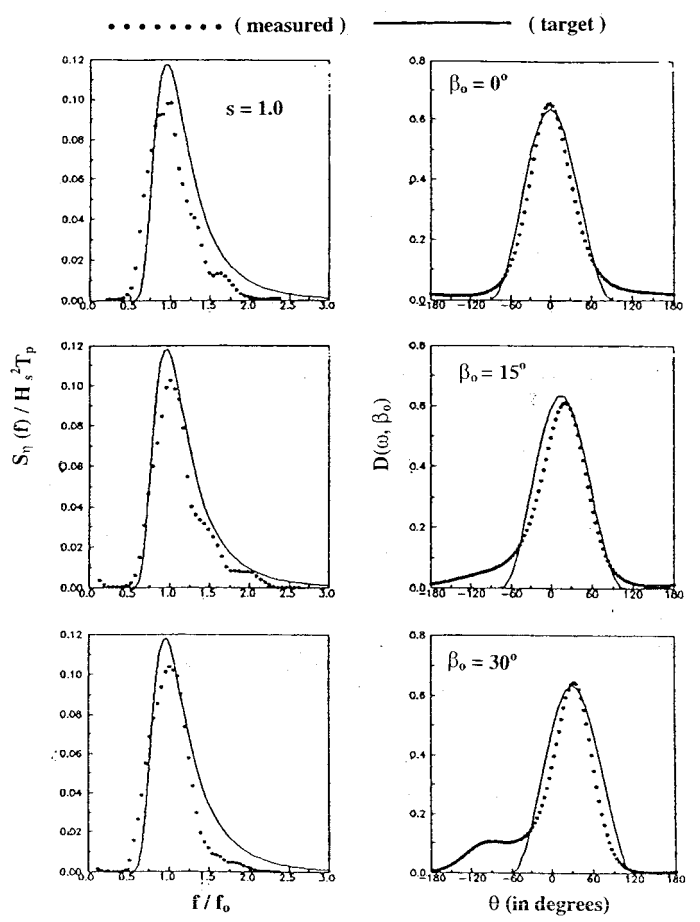


Fig. 6 Comparison of measured and target frequency spectra and directional spread for different β (without cylinder).

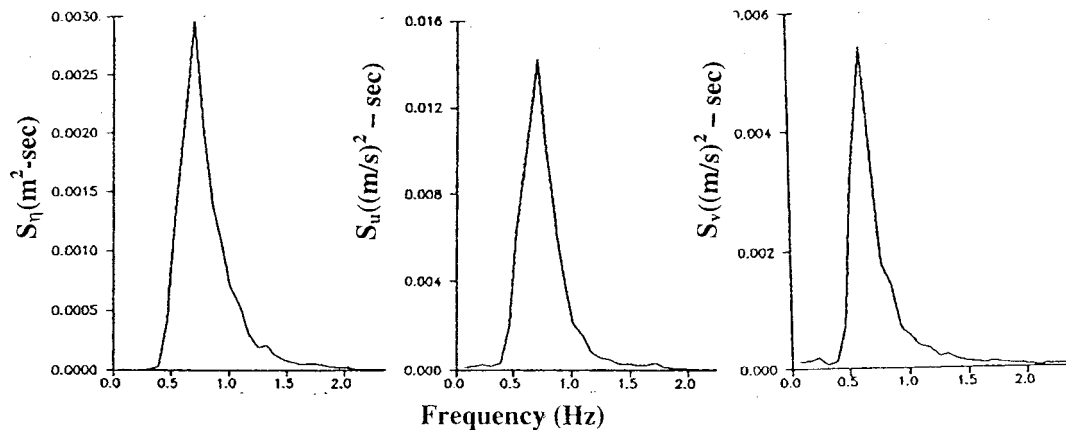


Fig. 7 Spectral density variation of water surface elevation, in-line transverse Velocities.

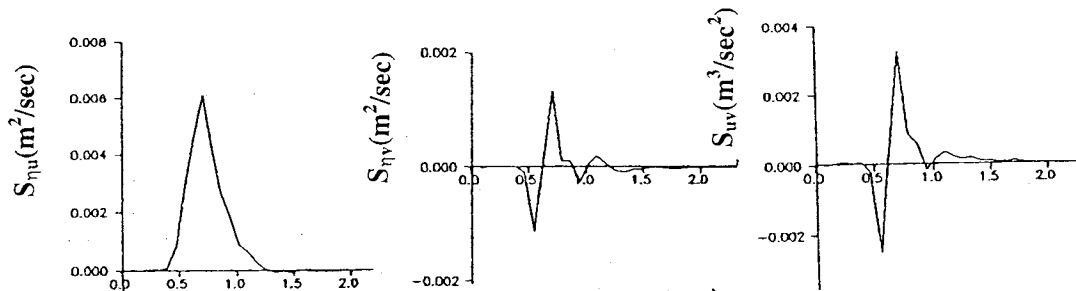


Fig. 8 Co-spectral density of in-line, transverse velocities and co-spectra of velocities in in-line and transverse directions.

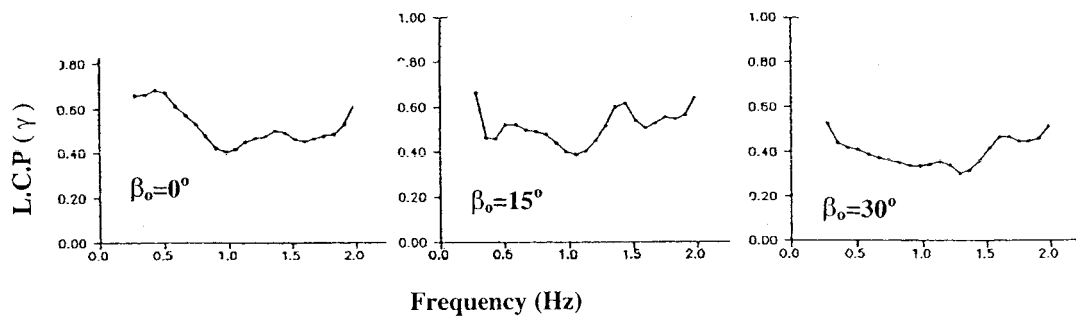


Fig. 9 Variation of long crested parameter with frequency for different mean wave directions.

frequency) is plotted against the normalized frequency f^* ($f^* = f/f_0$) shows a good comparison. Similarly the comparison between the measured the target directional spread, $D(\omega, \beta)$ is found to be quite satisfactory. The deviation of measured spread increases with increase in the mean wave direction. The possible reason for this discrepancy is due to the reflection from the absorbers, as well as from the LCWM.

4.2 Average Spectral Characteristics

The characteristics of spectra for the different associated variables with the directional waves, viz., the wave spectra, $S_\eta(f)$, in-line velocity spectra $S_u(f)$, transverse velocity spectra $S_v(f)$, co-spectra (η and u), $S_{\eta u}(f)$, co-spectra (η and v), $S_{\eta v}(f)$ and co-spectra (u and v), $S_{uv}(f)$ for the run defined by DW1 and $\alpha = -15^\circ$ are reported in Figs. 7 and 8 respectively. The peaks of all the spectra

are seen to occur at the same frequency. The transverse velocity spectral peak for this particular test is observed to be nearly 50 percent of the in-line velocity spectral peak. The shape of the three auto spectra of η , u and v are observed to be similar. The $S_{\eta u}$ spectrum indicates that negative values are almost negligible, whereas the variation of $S_{\eta u}$ and S_{uv} are found to be similar.

The variation of the long crested parameter, γ discussed by Kobune et al., (1985) for $\alpha = -15^\circ$ subjected to the wave characteristics DW1 ($\beta_0 = 0^\circ$), DW2 ($\beta_0 = 15^\circ$) and DW3 ($\beta_0 = 30^\circ$) are shown in Fig. 9. The results indicate that in all cases γ varies from about 0.3 to 0.7. It also indicates that as the mean direction increases, γ at peak frequency is found to reduce, showing that a more short crested sea is observed for a higher value of mean wave direction.

It was found that irrespective of the mean wave direction the change in the standard deviation as a function of frequency was

not significant. Similarly the variation of skewness and kurtosis as a function of frequency did not exhibit a regular trend with the change in the mean direction. In order to make the presentation simple these results are avoided in this paper.

4.3 Pressure ratio

Typical incident wave spectra and the pressure spectra around the cylinder for the LCW and that for DW1 for $\alpha = -15^\circ$ are shown in **Fig.10**. The results show that even a smaller percentage of variation in the wave spectra results in a larger percentage of differences in the pressure spectra around cylinder. The shape of the spectra for the two kinds of waves tested found to be similar.

The average spectral characteristics of the waves generated for the different angles of inclination of the cylinder namely, peak frequency, f_o , peakedness parameter, γ_1 , narrowness parameter, γ_2 , spectral width parameter, ϵ , and significant wave height, H_s , are reported in Tables. 2 to 4.

The various parameters, peakedness parameter (γ_1) and narrowness parameter (γ_2) are defined as

$$\text{Peakedness parameter: } \gamma_1 = \frac{2}{m_o^2} \int \{S(f)\}^2 df \quad (3)$$

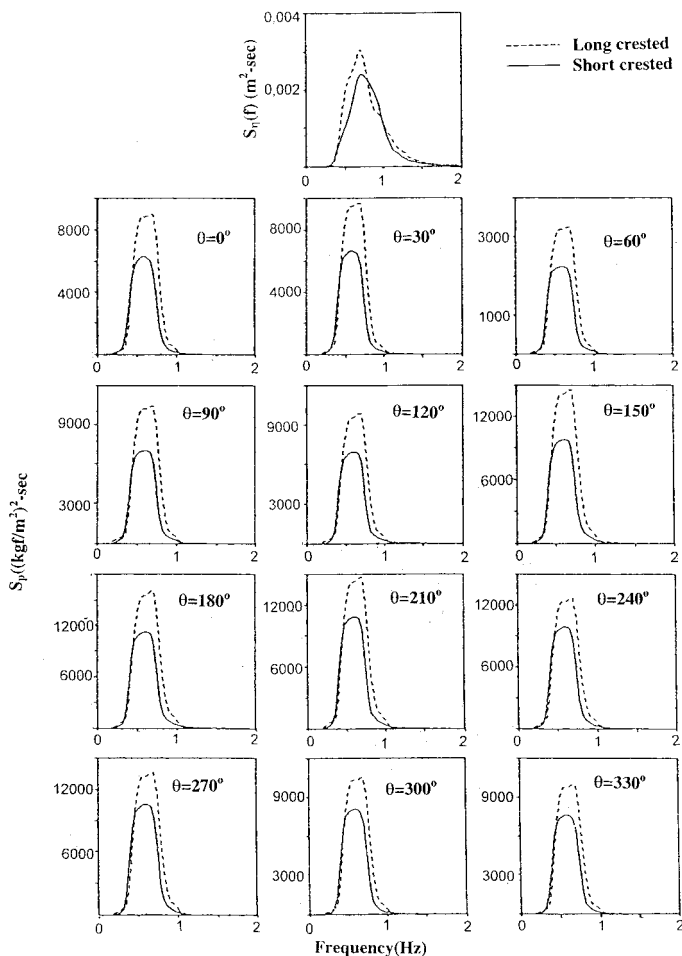


Fig. 10 Typical wave spectra and the pressures spectra for the long crested wave and for the short crested waves.

$$\text{Narrowness parameter: } \gamma_2 = \sqrt{\frac{m_o m_2 - m_1^2}{m_1^2}} \quad (4)$$

Table 2. Average spectral characteristics of $\eta(t)$ for angle of inclination $\alpha = \pm 15^\circ$

Wave	$\alpha = 15^\circ$					$\alpha = -15^\circ$				
	f_o	γ_1	γ_2	ϵ	H_s (m)	f_o	γ_1	γ_2	ϵ	H_s (m)
LCW	0.66	2.8	0.24	0.48	0.18	0.66	2.88	0.26	0.52	0.19
DW1	0.72	2.35	0.27	0.51	0.13	0.72	2.38	0.26	0.50	0.14
DW2	0.76	2.15	0.28	0.52	0.11	0.61	2.06	0.28	0.52	0.12
DW3	0.80	2.38	0.25	0.48	0.11	0.76	2.43	0.25	0.47	0.11

Table 3. Average spectral characteristics of $\eta(t)$ for angle of inclination $\alpha = \pm 30^\circ$

Wave	$\alpha = 30^\circ$					$\alpha = -30^\circ$				
	f_o	γ_1	γ_2	ϵ	H_s (m)	f_o	γ_1	γ_2	ϵ	H_s (m)
LCW	0.64	2.78	0.24	0.48	0.18	0.66	2.87	0.27	0.53	0.19
DW1	0.64	2.29	0.27	0.50	0.14	0.72	2.33	0.26	0.49	0.14
DW2	0.74	2.23	0.27	0.52	0.11	0.61	2.05	0.28	0.52	0.12
DW3	0.80	2.23	0.25	0.47	0.11	0.76	2.40	0.26	0.48	0.11

Table 4. Average spectral characteristics of $\eta(t)$ for angle of inclination $\alpha = \pm 45^\circ$

Wave	$\alpha = 45^\circ$					$\alpha = -45^\circ$				
	f_o	γ_1	γ_2	ϵ	H_s (m)	f_o	γ_1	γ_2	ϵ	H_s (m)
LCW	0.64	2.74	0.25	0.49	0.18	0.66	2.90	0.27	0.54	0.18
DW1	0.64	2.31	0.28	0.52	0.13	0.64	2.40	0.27	0.50	0.14
DW2	0.78	2.28	0.28	0.52	0.12	0.74	2.20	0.29	0.54	0.12
DW3	0.80	2.34	0.25	0.46	0.11	0.76	2.40	0.25	0.46	0.11

The tables 2 to 4 shows that the incident wave spectra for all the tests are narrow banded.

The p_r around the cylinder for different α and subjected to waves with different β_o are shown in Fig. 11. The p_r for $\alpha = 15^\circ$ at $\theta = 0^\circ$ is found to be slightly greater than unity, indicating that the pressure at this location due to 3D waves is slightly greater than that due to 2D waves. The average percentage of variation in p_r around the circumference of the cylinder is approximately 6%. The p_r for the test conditions $\beta_o = 15^\circ$ and 30° is found to be about 15 to 20% greater than the p_r for the cylinder subjected to directional waves with $\beta_o = 0^\circ$. Similar results are obtained for $\alpha = -15^\circ$. In contrary to what was obtained for the earlier case the p_r for the directional waves with mean direction $\beta_o = 15^\circ$ is always found to be greater than 1.0 all around the circumference. The effect of mean direction is seen all around the circumference. The p_r for $\beta_o = 15^\circ$ is about 10-15 percent higher than that obtained for $\beta_o = 0^\circ$. Summarizing the above for $\alpha = \pm 15^\circ$, the directional waves with mean direction of 15° exert a larger force compared to that due to 3D waves with mean directions of 0° and 30° . The p_r for $\alpha = +30^\circ$ is least for $\beta_o = 0^\circ$, whereas for the other two β_o values, the p_r has about the same magnitude. This is almost similar to the results that were obtained for $\alpha = +15^\circ$. However, for

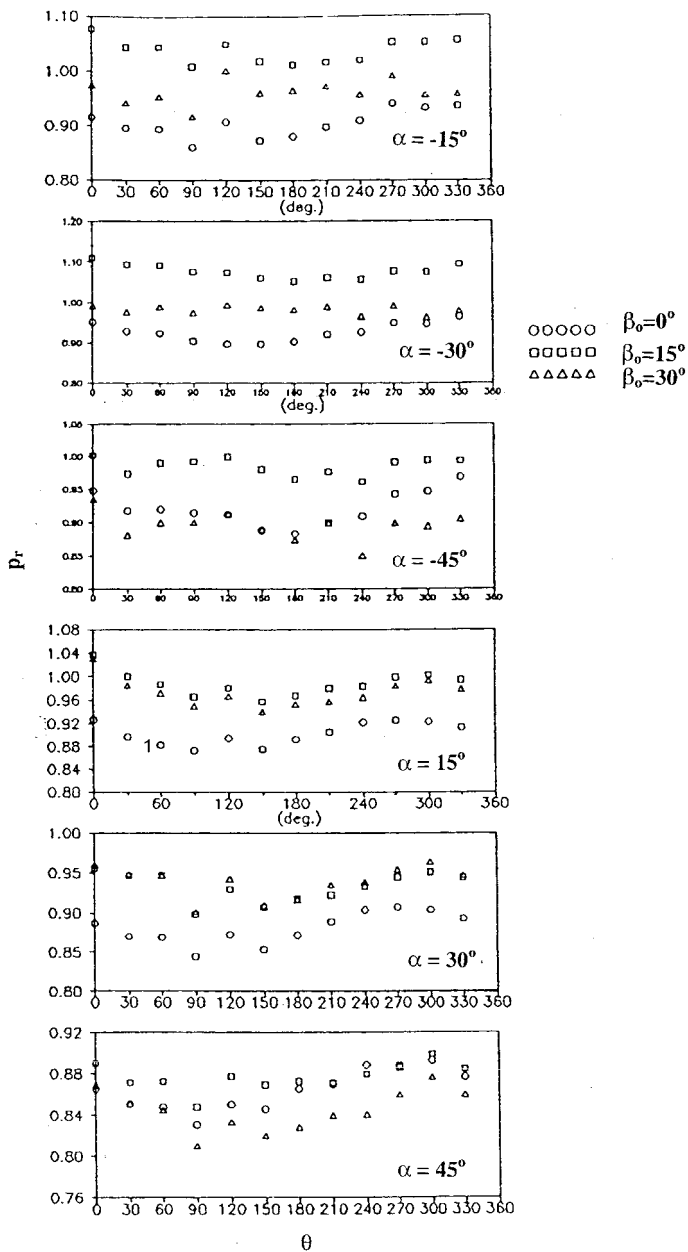


Fig. 11 Circumferential variation of pressure ratio with α .

this condition the p_r for all the β_0 tested is found to be less than one. For the case of $\alpha = -30^\circ$ the p_r is always found to be greater than one for mean direction, $\beta_0 = 15^\circ$ and is found to be highest comparing the three wave directions tested. For the condition $\alpha = \pm 45^\circ$, it is again observed that $\beta_0 = 15^\circ$ offers maximum p_r all around the circumference and it is found to be less than 1.0. If one compares all the α tested, it can be interpreted that when $\alpha = \pm 45^\circ$ the cylinder experiences minimum p_r around its circumference. For $\beta_0 = 30^\circ$ and when $\alpha = -30^\circ$ exposed to directional waves with a mean direction of 15° , the p_r is found to be the highest.

4.4 Force Spectra

A typical plot showing the normal force spectrum $S_{fn}(f)$, in-line force spectrum $S_{fx}(f)$, transverse force spectrum $S_{fy}(f)$ and vertical force spectrum $S_{fz}(f)$ obtained for the cylinder inclined at 15°

against the wave direction ($\alpha = -15^\circ$) and subjected to a directional wave spectrum, DW1 are shown in Fig. 12. The target and measured $S_{\eta}(f)$ is already reported. It is observed that the shape of the force spectrum is similar to the wave spectrum and the peak energy is observed to occur at the same frequency. For this angle of inclination of the cylinder, the peak energy of the normal sectional force f_n is almost of same magnitude as that of the in-line force, f_x . The transverse force is observed to be about half the normal force, whereas the vertical force f_z is only to the extent of about 7 percent of the normal force.

The average spectral characteristics ($\gamma_1, \gamma_2, \epsilon$) of force time histories, $f(t)$ are presented in Tables. 5 to 7 for $\alpha = \pm 15^\circ, \pm 30^\circ$ and $\pm 45^\circ$ respectively. The characteristics of long crested random wave (LCW) are also included in this table. The value of ϵ of the force spectra or all the type of waves is found to be close to that of wave spectra, even for LCW. It may be recalled that for the tests done with random waves with a much lower value of H_s resulted in a higher value for ϵ for the force spectra.

Table 5. Average spectral characteristics of $f(t)$ for angle of inclination $\alpha = \pm 15^\circ$

Wave	$\alpha = + 15^\circ$					$\alpha = - 15^\circ$					
	Type	f_0	γ_1	γ_2	ϵ	Sig. value (N)	f_0	γ_1	γ_2	ϵ	Sig. value (N)
LCW		0.66	3.66	0.15	0.29	34.40	0.64	3.48	0.16	0.30	37.00
DW1		0.63	3.42	0.17	0.32	19.10	0.61	3.30	0.18	0.30	20.50
DW2		0.61	3.02	0.18	0.34	20.40	0.70	3.00	0.18	0.30	21.30
DW3		0.61	2.78	0.20	0.36	17.90	0.61	2.70	0.20	0.38	20.00

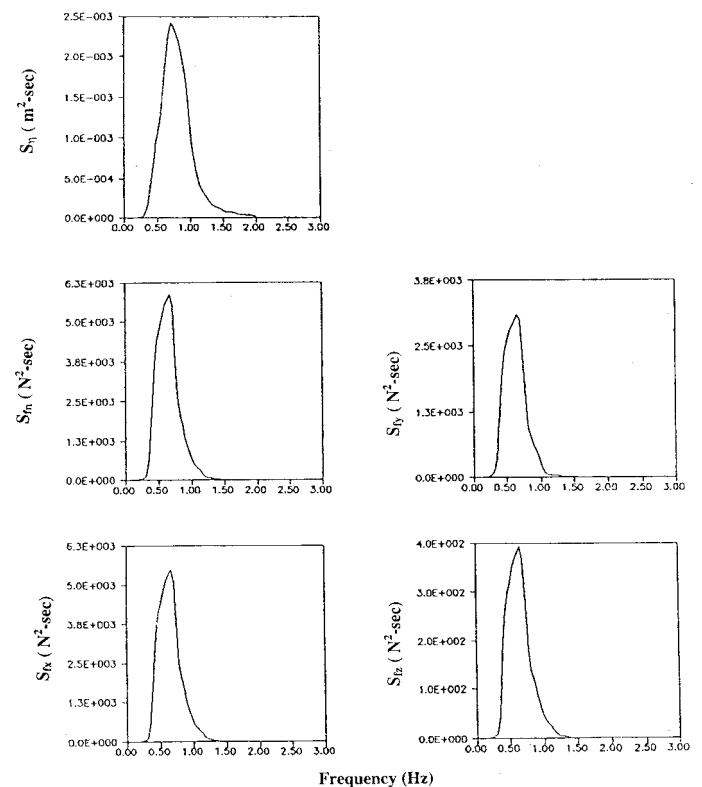


Fig. 12 Typical plot of surface elevation and force spectra (for tests DW1 and $\alpha = -15^\circ$)

Table 6. Average spectral characteristics of $\eta(t)$ for angle of inclination $\alpha = \pm 30^\circ$

Wave	$\alpha = +30^\circ$					$\alpha = -30^\circ$				
	f_o	γ_1	γ_2	ϵ	Sig. value (N)	f_o	γ_1	γ_2	ϵ	Sig. value (N)
LCW	0.66	3.60	0.16	0.29	33.60	0.64	3.54	0.16	0.30	37.70
DW1	0.63	3.40	0.17	0.32	18.90	0.61	3.20	0.19	0.35	20.90
DW2	0.61	3.00	0.18	0.34	20.00	0.70	3.00	0.18	0.33	22.30
DW3	0.61	2.78	0.20	0.36	17.70	0.61	2.70	0.20	0.38	20.20

Table 7. Average spectral characteristics of $\eta(t)$ for angle of inclination $\alpha = \pm 45^\circ$

Wave	$\alpha = 45^\circ$					$\alpha = -45^\circ$				
	f_o	γ_1	γ_2	ϵ	Sig. Value (N)	f_o	γ_1	γ_2	ϵ	Sig. Value (N)
LCW	0.64	3.40	0.17	0.31	34.70	0.66	3.70	0.15	0.29	38.10
DW1	0.63	3.20	0.18	0.35	20.50	0.61	3.30	0.18	0.34	21.80
DW2	0.72	3.00	0.19	0.35	20.50	0.63	3.10	0.18	0.34	23.70
DW3	0.61	2.70	0.20	0.38	18.90	0.64	2.70	0.20	0.37	20.50

In this section, the variation of the spectral density of the normal and its components in x, y and z directions with mean direction are discussed. Fig. 13 shows the variation of normal force spectra with mean direction. It is observed that for $|\alpha| \leq 30^\circ$, the effect of mean direction on the wave force spectral peak is found to be less. Further increase in α as in the case for $\alpha = \pm 45^\circ$, the normal force spectral peak is found to increase for negative α . For all α ,

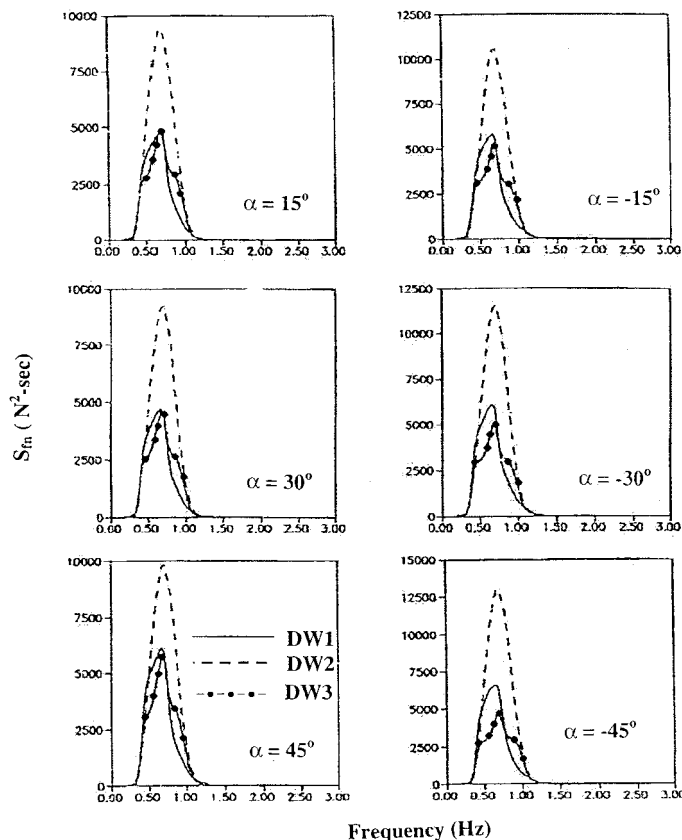


Fig. 13 Effect of mean wave directions on the normal force spectra.

the normal force exerted by directional waves with mean direction of 15° results in higher normal forces. Further, the normal force spectral peak obtained with mean directions 0° and 30° are almost same for $+\alpha$, whereas, the normal force spectral peak due to directional waves with mean direction of 0° is found to be greater than that due to results obtained with $\beta_o = 30^\circ$. These results are seen for negative α .

The effect of the mean wave direction on in-line force spectra is presented in Fig. 14. The variation is similar to that of normal force spectra for all α and β .

The effect of mean wave directions on transverse force spectra and vertical force spectra are shown in Figs. 15 & 16 respectively. As β_o increases from 0° to 30° (DW1 to DW3), the spectral peak of the transverse force is reduced; the reduction of the spectral peak for $\beta_o = 0^\circ$ to 15° is more and the reduction from $\beta_o = 15^\circ$ to 30° is less for all increases of cylinder inclinations along the wave direction studied. For the cylinders inclined against wave direction, the reduction of spectral peak being less from $\beta_o = 0^\circ$ to 15° compared to reduction between $\beta_o = 15^\circ$ to 30° .

The magnitude of transverse force is equal in the corresponding positive and negative inclinations for DW1 and DW3. For the case of DW2, a significant difference in force spectral peak is observed for positive and negative α , which may be due to the wave field conditions in the wave basin as discussed earlier. The variation of vertical force spectra is similar to that obtained for normal and in-line force spectra for all the cases tested.

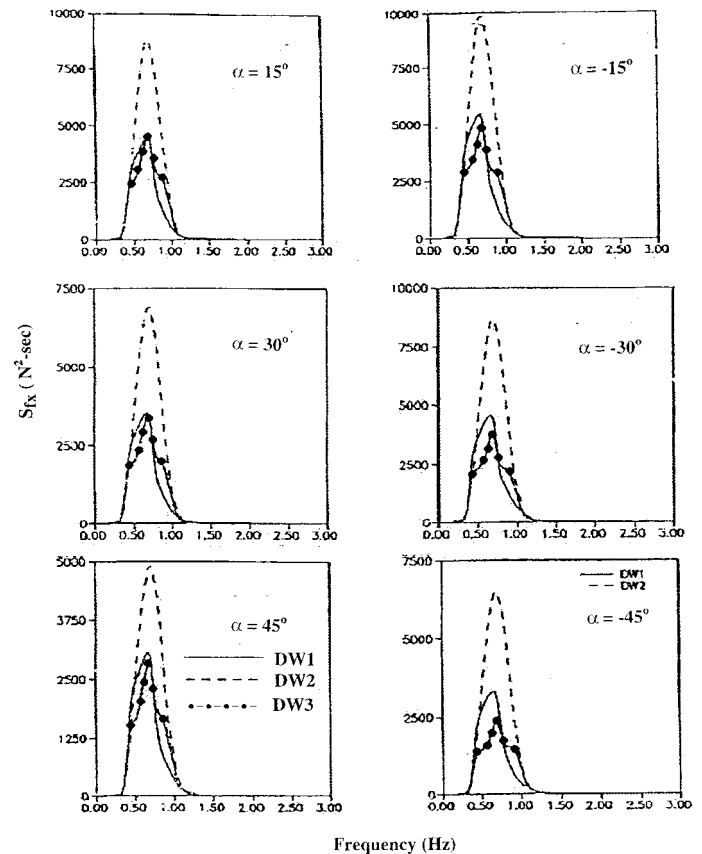


Fig. 14 Effect of mean wave directions on the in-line force spectra.

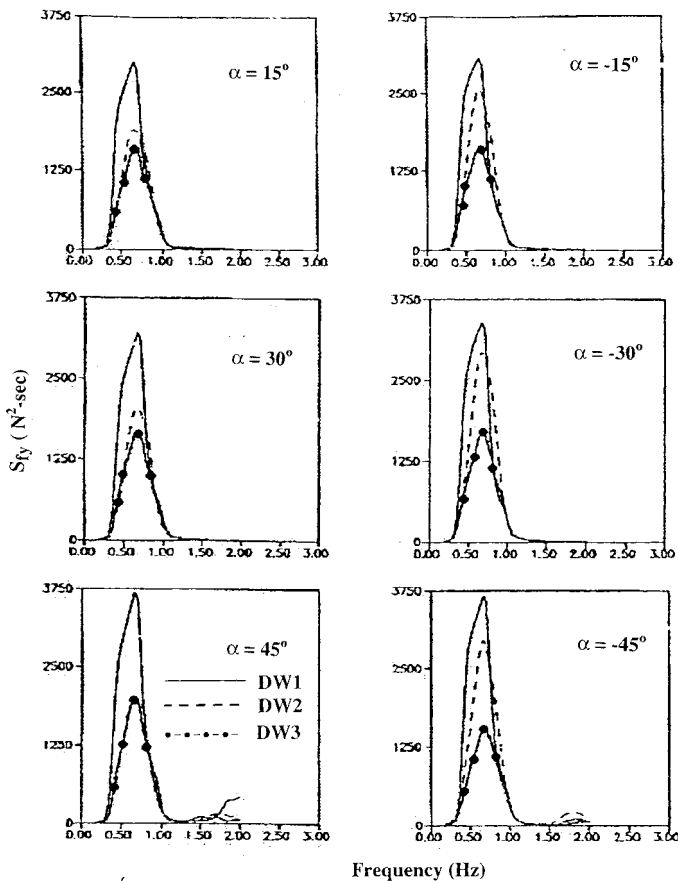


Fig. 15 Effect of mean wave directions on the transverse force spectra.

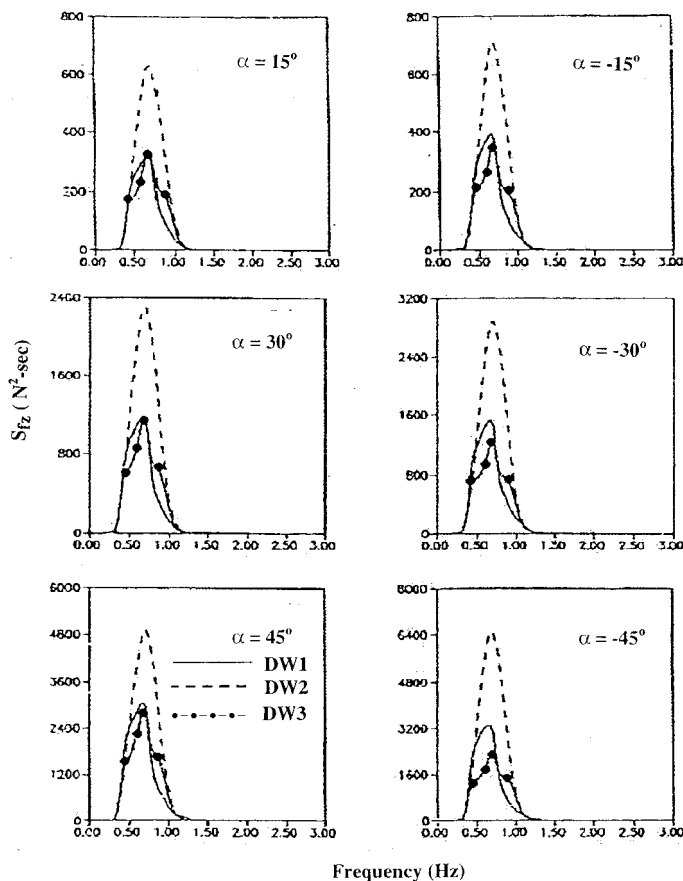


Fig. 16 Effect of mean wave directions on the vertical force spectra.

4.5 Force ratio

The variation of normal force ratio with different β_0 is shown in Fig. 17. The results indicate that, for $-\alpha$, $[f_r]_n$ is found to generally increase in β_0 , whereas, for $+\alpha$, the force ratio for $\beta_0 = 15^\circ$ is observed to be higher than that obtained for $\beta_0 = 30^\circ$. This trend is not significant for $\alpha = +45^\circ$. If one considers $\beta_0 = 0^\circ$, the values of the $[f_r]_n$ for all α , range between 0.8 and 0.85, thus indicating that the forces on an inclined cylinder due to 3D waves is about 15-20 percent less than that due to 2D waves. The $[f_r]_n$ values for the vertical cylinder subjected to directional waves with $\beta_0 = 0^\circ$ and 15° exhibit the least force, about 20 percent less than that due to long crested waves, closer to the observations of Chaplin et al. (1993). The variation of in-line force ratio $[f_r]_x$ is depicted in Fig. 18. These results are similar to that observed for $[f_r]_n$. A maximum reduction of about 22.5 percent is observed for $\alpha = -15^\circ$ with $\beta_0 = 0^\circ$. While the in-line force in a directional wave field is observed equal to the force in a long crested wave field for $\alpha = -30^\circ$ and $\beta_0 = 30^\circ$. In general, as α increases, along and against the wave directions, the force ratio increases for DW2 and is found to decrease for DW3.

The transverse force ratio for the different cylinder inclinations in different directional homogeneous waves with $\beta = 0^\circ, 15^\circ, 30^\circ$ is presented in Fig. 19. It is observed that the transverse force ratio in a directional wave field is larger than in a long crested wave field. A value of the transverse force ratio of more than 2 is observed for $\alpha = +45^\circ$ with $\beta = 0^\circ$, that is, the transverse force exerted on the cylinder in a directional wave field is twice that of forces experienced in a long crested wave field. In general, the force ratio decreases with increase in β_0 . The transverse force ratio is observed to be in a narrower range for negative α (cylinder inclined against the wave direction), while range of force ratio is more for positive α . The transverse force experienced in a directional wave field is observed to have minimum amplification of 1.25 times, the transverse force experienced due to the action of long crested wave field. This aspect greatly affects the design aspects in a sectional level rather than in the total force estimation.

The variation of vertical force ratio with β_0 for various inclinations of cylinder is presented in Fig. 20. The vertical force ratio increases with mean wave direction for $\alpha = -15^\circ, -30^\circ$. A signifi-

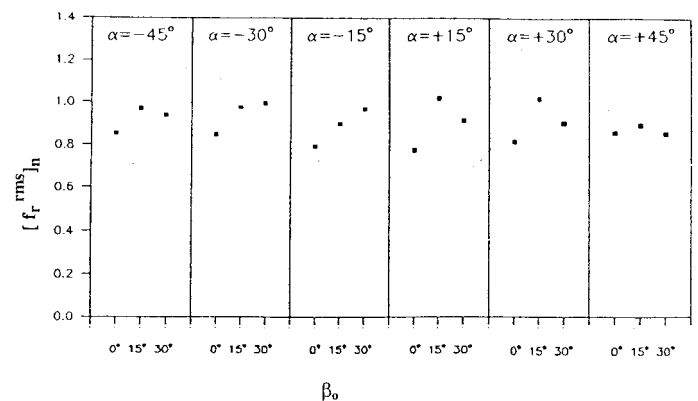


Fig. 17 Variation of normal force ratio (rms) with the angle of inclination of cylinder for different mean wave directions.

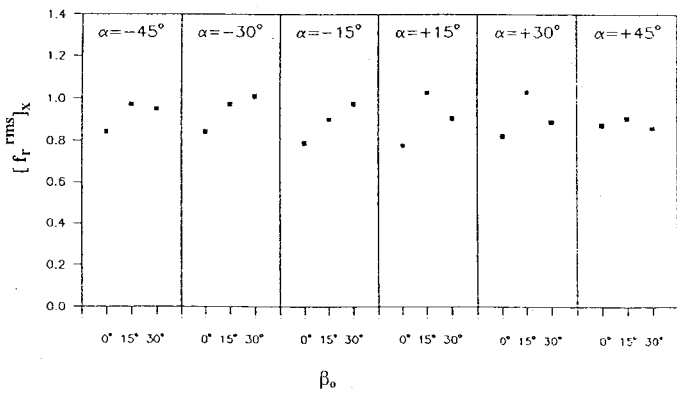


Fig. 18 Variation of in-line force ratio (rms) with the angle of inclination of cylinder for different mean wave directions.

cant difference in force ratio for the cases of $\beta_0 = 0^\circ$ and 30° is observed for negative α , while the difference is quite narrow for positive α (DW1 and DW3). A maximum reduction in vertical force of 27 percent is observed for $\beta_0 = 30^\circ$ and $\alpha = +15^\circ$.

For $\alpha = -30^\circ$ the vertical force in directional wave field is observed to be the same as for force in a long crested wave field under the action of directional wave with $\beta = 30^\circ$. This also observed for the normal force and the in-line force.

It is, in general, observed that the magnitude of the normal force does not vary significantly with α , while a gradual reduction in the magnitude of in-line force is observed with increase in the angle of orientation when it is inclined both along and against the wave direction. This is due to the effect that even though the magnitude of normal force is almost the same for all the inclinations of cylinders, the distribution of the force component along the x, y and z directions is significantly altered due to the cylinder inclination. The in-line force is observed to increase with decrease in α ($\alpha = -45^\circ$ to -15° and ($\alpha = +45^\circ$ to $+15^\circ$). The vertical force is observed to increase with increase in α with cylinder inclined along and against the wave directions is a directional wave field. In order to define the maximum force occurring on the cylinder, the magnitude of the maximum force obtained from the statistical analysis of the force trace is presented by normalizing with rms wave height. The results of normalized maximum force in a directional wave field are compared to a maximum force exerted in a long crested wave field. The maximum force ratio (f_r^{\max}) is de-

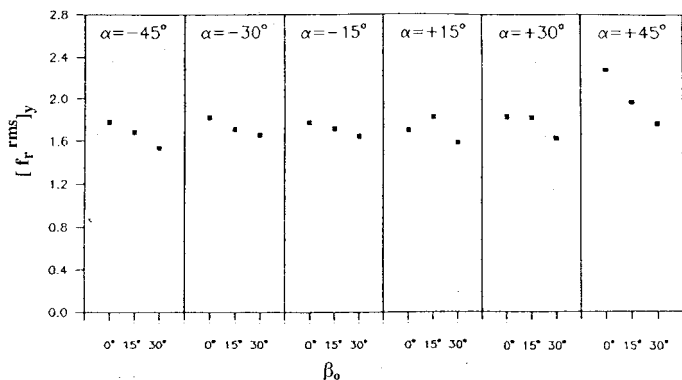


Fig. 19 Variation of transverse force ratio (rms) with the angle of inclination of cylinder for different mean wave directions.

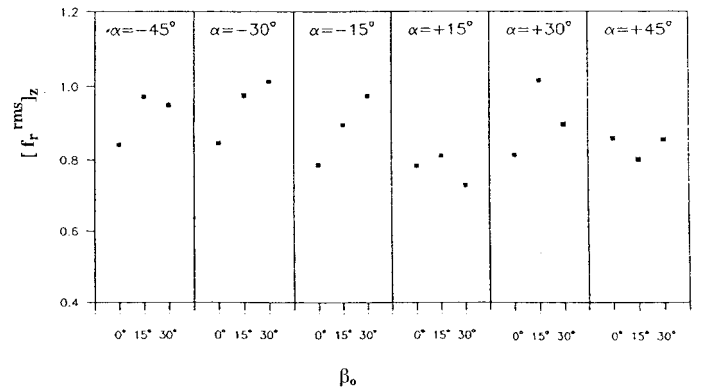


Fig. 20 Variation of vertical force ratio with angle of inclination of cylinder of different mean wave directions.

finied as

$$f_r^{\max} = \frac{\left[\frac{f_{\max}^*}{H_{rms}} \right]_{3D}}{\left[\frac{f_{\max}^*}{H_{rms}} \right]_{2D}} \quad (5)$$

The maximum normal force ratio for all α for different β is presented in Fig. 21. The general trend is that the force ratio increases in β_0 ; however, as stated earlier, characteristics of waves in the basis are also governed by β_0 . So, we observe a high value of force ratio for $\beta_0 = 15^\circ$ than that for $\beta_0 = 30^\circ$. This is the trend seen for all the α tested.

A maximum force reduction of 25 percent to 37 percent is observed for directional wave fields with $\beta_0 = 0^\circ$ and with $\beta_0 = 30^\circ$ this reduction varies up to about 22 percent compared to the force experienced by the structure in 2D waves. For the tests done with $\beta_0 = 15^\circ$, the results show that force in the 3D waves increases by about 10 to 20 percent compared to that obtained for 2D waves. The variation of maximum in-line force ratio shown in Fig.22 exhibits a force reduction of 20 to 32 percent for the directional wave fields with $\beta_0 = 0^\circ$, 10 to 20 percent for a directional wave effect with $\beta = 30^\circ$; whereas for the tests with $\beta_0 = 15^\circ$, an increase in the forces due to 3D waves by about 10 to 20 percent compared to that due to 2D waves is observed. It is noted that the possible reduction in forces in directional waves helps the de-

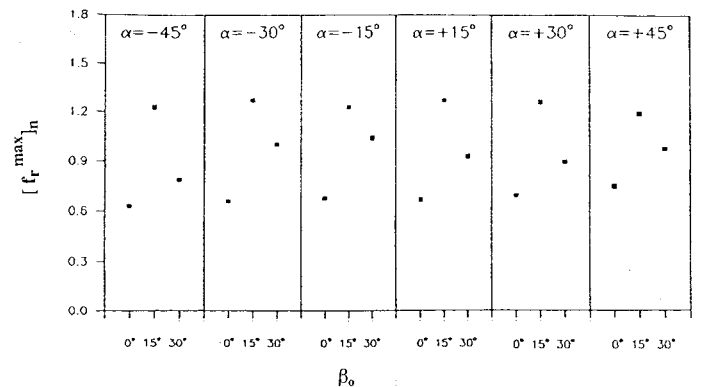


Fig. 21 Variation of maximum normal force ratio with angle of inclination of cylinder for different mean wave directions.

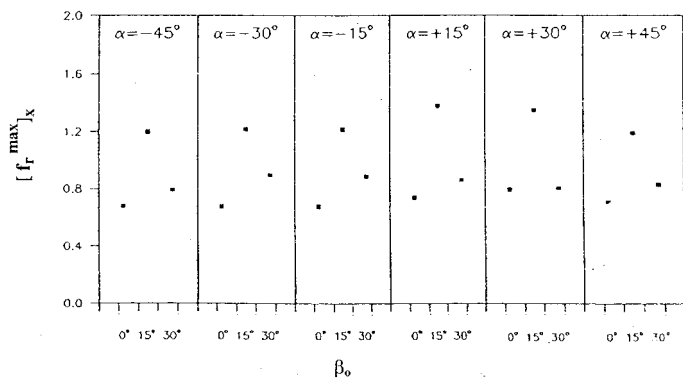


Fig. 22 Variation of maximum in-line force ratio with the angle of inclination of cylinder for different mean wave directions.

signer to optimize the design process.

The variation of maximum transverse ratio in different directional wave fields for different α is shown in Fig.23. As observed, the maximum force ratio is always greater than unity, indicating that the maximum transverse force in a directional wave field is always greater than that in a long crested wave field. A maximum amplification of about twice the force in a long crested wave field is observed for the case $\alpha = +45^\circ$ subject to DW1. It is worth nothing that, for the same test run, the rms transverse force ratio is in the order of 1.2 to 2.2. The transverse maximum force ratio is found to decrease with increase in β_0 for all α . The rate of decrease is more for $\alpha = -45^\circ$ and $\alpha = +45^\circ$ and least for $\alpha = -15^\circ$ and $+15^\circ$.

The variations of maximum vertical force with mean wave directions for different α is depicted in Fig.24. The trend in its variation with β_0 for all α is similar to that obtained for the normal and in-line maximum force ratio. A reduction of 25 to 32 percent is observed in a directional wave field with $\beta_0 = 0^\circ$ and in a directional wave field $\beta_0 = 30^\circ$, the reduction is in the order of 3 to 20 percent. When the cylinder is subjected to directional waves with $\beta_0 = 15^\circ$, the maximum force ratio is found to be a maximum of about 1.2 for all α except for $\alpha = +45^\circ$. The reduction is observed to be more for cylinders inclined against the wave direction compared to the cylinders inclined along the wave direction.

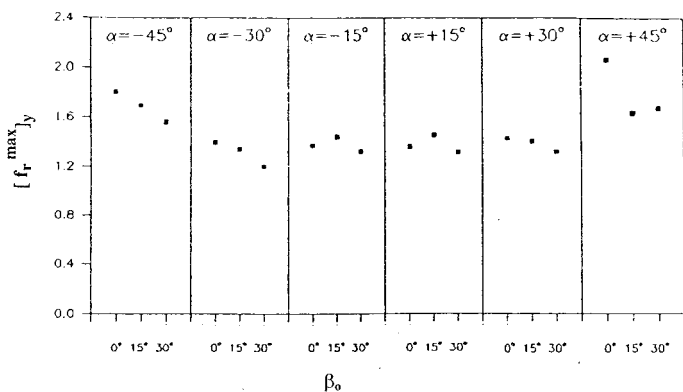


Fig. 23 Variation of maximum transverse force ratio with the angle of inclination of cylinder for different mean wave directions.

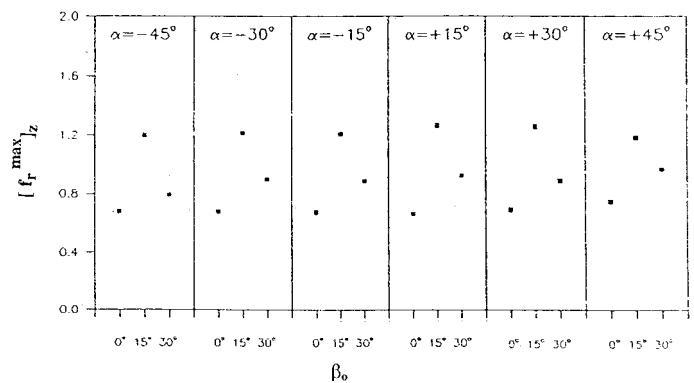


Fig. 24 Variation of maximum vertical force ratio with the angle of inclination of cylinder for different mean wave directions.

5. Summary and conclusions

The effect of directional waves on the pressure distribution around the circumference of the cylinder as compared to the uni-directional random waves is observed to decrease the spectral density of the pressures measured.

The average percentage variation in the pressure of short crested wave as compared to the long crested wave (pressure ratio) around the circumference of the cylinder is approximately 6 percent. The pressure ratio for the test conditions, with mean wave direction, $\beta_0 = 15^\circ$ and 30° is found to be 15 to 20 percent greater than the pressure ratio exerted on the cylinder with mean wave direction of 0° . It is also observed that for $\alpha = 45^\circ$, the cylinder experiences minimum pressure ratio.

In short crested waves, it is observed that the variation of spectral peak of normal force is found to increase in angle of orientation of the cylinder as mean wave direction increases. It is also seen that the normal force peak is higher for a particular angle of orientation, when inclined against the direction of wave.

The in-line force spectra in a directional wave is observed to decrease with increase in angle of orientation of the cylinder for $\beta_0 = 0^\circ$ to 30° , whereas the variation of transverse and vertical force spectra is observed to increase with increase in angle of orientation of the cylinder for $\beta_0 = 0^\circ$ to 30° .

The effect of mean wave direction, for $\beta_0 = 15^\circ$, on the spectral peaks of normal, in-line and vertical forces is observed to be considerably higher than that due to the mean wave directions β_0 of 0° to 30° . The spectral peak of transverse force is observed to decreasing for $\beta_0 = 0^\circ$ to 30° for all the angle of inclination of the cylinder tested along and against the direction of the waves.

The rms value of normal and in-line force of short crested wave as compared to a long crested wave is found to increase with mean wave direction ranging from $\beta_0 = 0^\circ$ to 15° and is found to decrease in the range of 15° to 30° . A maximum reduction of 22.5 percent is observed for the cylinder orientation $\alpha = 0^\circ$, for $\beta = 0^\circ$. The transverse force ratio in the directional wave field is found to be larger than in the long crested wave field. This ratio is found to decrease with increase in the mean wave direction. A minimum value of 1.25 is observed for the vertical cylinder and a maximum amplification of 2.3 is observed for $\alpha = 15^\circ$.

The trend in the variation of vertical force ratio is observed to be

similar to that of the normal and in-line force ratios. A reduction of about 27 percent is observed in directional waves as compared to long crested waves for $\alpha = 15^\circ$.

The maximum normal force ratio is observed to have a reduction of 25 percent to 37 percent for a directional wave field as compared to a long crested wave field with $\beta_0 = 0^\circ$. For the mean wave direction, $\beta_0 = 30^\circ$, this reduction is observed to vary up to about 22 percent. The ratio for the mean wave direction, for $\beta_0 = 15^\circ$, shows that the force in the 3D waves increases by about 10 to 20 percent compared to that obtained for 2D waves a similar trend is observed for the maximum in-line force ratio.

The amplification of the maximum transverse force ratio is observed to be of the order of 1.2 to 2.2 for the various mean waves directions tested. The variation of maximum vertical force ratio with mean wave direction for an inclined cylinder is observed to show a reduction of 20-32 percent in a directional wave field as compared to a long crested wave field.

Acknowledgements

The work presented here is a part of the sponsored project funded by the Volkswagen Research Foundation and Deutsche Gesellschaft fuer Technische Zusammenarbeit (GTZ), Germany. The authors wish to express their sincere thanks to the Head of the Department of Ocean Engineering, Indian Institute of Technology, Madras, India, for providing all the experimental facilities. The authors thank Professor H.Kaldenhoff, Bergische Universitaet, Wuppertal, Germany, for his suggestions during the course of this study.

References

AAGE, C., JORGENSEN, P., ANDERSON, W., DAHL KLINTING, P. (1989) Wave loads on a cylinder in 2-D and 3-D deep water waves, Proceedings of the *Eight International Conference, Offshore Mechanics and Arctic Engineering*, The Hauge, 175-181.

ANANDKUMAR, G., SUNDAR, V., GRAW, K.U. and KALDENHOFF, H. (1995a) Pressures and Forces on Inclined Cylinders due to Regular Waves. *Ocean Engineering*, 22, 747-759.

ANANDKUMAR, G., SUNDAR, V., GRAW, K.U. and KALDENHOFF, H. (1995b) Wave loads on inclined cylinders due to random waves. Proceedings of *Fifth International Offshore and Polar Engineering Conference*, The Hauge, The Netherlands, 221-226.

BORGMAN, L.E. (1958) Computation of ocean wave forces on inclined cylinders, *Transactions American Geophysical Union*, vol.39, No.5.

CHAKRABARTI, S.K., WOLBERT, A.I. and TAM, W.A. (1977) Wave forces on Inclined Tubes, *Coastal Engineering*, 1, 149-165.

CHAPLIN, J.R., SUBBIAH, K. and IRANI, M. (1993). Effects of wave directionality on the In-line loading of a vertical cylinder. Proceedings of *Third International Offshore and Polar Engineering Conference*, Singapore, 116-120.

HOGEDAL, M., SKOURUP, J. and BUCHARTH, H.F. (1994) Wave

force on vertical smooth cylinder in directional waves, Proceedings of *Fourth International Offshore and Polar Engineering Conference*, Osaka, Japan, 218-223.

ISOBE, M., KONDO, K. and HORIKAWA, K. (1984) Extension of MLM for estimating directional wave spectrum. Symposium on *Description and Modelling for Directional Seas*, Technical University, Denmark, June, A6-1-A6-15.

ISSACSON, M. and NWOGU, O. (1988) Short-crested wave forces on a vertical pile, Proceedings of *Offshore Mechanics and Arctic Engineering*, Houston 2, 47-54.

JOHANSSON, P.I. (1978) *Ocean Test Structure Data Interpretation*, Part 4-Task – II-C, Det Norske Veritasm, Report 78-531.

MILES, M.D. (1990) Numerical models for synthesis of directional seas. Report No. TR-HY-016, National Research Council, Canada.

MORISON, J.R., O'BRIEN, M.P., JOHANSON, J.W. and SCHAAF, S.A. (1950). The force exerted by surface waves on piles, *Petroleum Transactions*, AIME, 189, 149-154.

NWOGU, O.U., MANSARD, E.P.D., MILES, M.D. and ISAACSON, M. (1987) Estimation of directional wave spectra by the maximum entropy method. Proceedings of IAHR Seminar, XXII congress, Lausanne, Switzerland, September, 363-376.

REID, R.O. (1957) Correlation of water level variations with wave forces on a vertical pile for non-periodic waves, Proceedings of the *Sixth International Coastal Engineering Conference*, Florida, 749-786.

SAND, S.E. and MYNETT, A.E. (1987) Directional wave generation and analysis. Proceedings of IAHR seminar, XXII Congress, Lausanne, Switzerland, September, 209-235.

SUNDAR, V., VENGATESAN, V., ANANDKUMAR, G. and SCHLENKHOFF, A. (1998) Hydrodynamic coefficients for inclined cylinder, *Ocean Engineering*, 25, 277-294.

Notation

C_D	Drag coefficient
C_M	Inertia coefficient
D	Diameter of cylinder
DW1, DW2 & DW3	Directional waves
FM	Fourier Series Method
f_r	Force ratio
f_n	Normal sectional force
f_x	In-line force
f_z	Vertical force
f(t)	Force time history
f_r^{\max}	maximum force ratio
H_s	Significant wave height
KC	Keulegan-Carpenter Number
LCW	Long crested random Waves
LCWM	Long Crested Wave Maker
MEM	Maximum Entropy Method
MEWM	Multi Element Wave Maker
MLM	Maximum Likelihood Method
p_r	Pressure ratio
rms	Root mean square
$S_{in}(f)$	Normal force spectrum

$S_{fx}(f)$	In-line force spectrum	u_{max}	Maximum In-line particle velocity
$S_{ft}(f)$	Transverse force spectrum	v	Transverse particle velocity
$S_{uu}(f)$	In-line velocity spectrum	w	Vertical particle velocity
$S_{ww}(f)$	Vertical velocity spectrum	s	Spreading index
S_{η}	Normalized spectral density of wave elevation	θ	Orientation of pressure transducers with wave direction
$S_{\eta}(f)$	Wave spectra	γ	Long crested parameter
T_{η}	Wave period	ϵ	Spectral width parameter
T_p	Peak period	γ_1	Peakedness parameter
β	Wave direction	γ_2	Narrowness parameter
β_o	Mean wave direction		
η	Wave elevation		
u	In-line particle velocity		